



HAL
open science

Mechanofluorochromic Difluoroboron β -Diketonates Based Polymer Composites: Toward Multi-Stimuli Responsive Mechanical Stress Probes

Benjamin Poggi, Elliot Lopez, Rémi Métivier, Laurence Bodelot, Clémence Allain

► **To cite this version:**

Benjamin Poggi, Elliot Lopez, Rémi Métivier, Laurence Bodelot, Clémence Allain. Mechanofluorochromic Difluoroboron β -Diketonates Based Polymer Composites: Toward Multi-Stimuli Responsive Mechanical Stress Probes. *Macromolecular Rapid Communications*, 2022, 43 (15), pp.2200134. 10.1002/marc.202200134 . hal-03799197

HAL Id: hal-03799197

<https://hal.science/hal-03799197v1>

Submitted on 5 Oct 2022

HAL is a multi-disciplinary open access archive for the deposit and dissemination of scientific research documents, whether they are published or not. The documents may come from teaching and research institutions in France or abroad, or from public or private research centers.

L'archive ouverte pluridisciplinaire **HAL**, est destinée au dépôt et à la diffusion de documents scientifiques de niveau recherche, publiés ou non, émanant des établissements d'enseignement et de recherche français ou étrangers, des laboratoires publics ou privés.

Mechanofluorochromic Difluoroboron β -Diketonates based Polymer Composites: Toward Multi-Stimuli Responsive Mechanical Stress Probes

Benjamin Poggi, Elliot Lopez, Rémi Métivier,* Laurence Bodelot,* and Clémence Allain*

Developing mechano-responsive fluorescent polymers that exhibit distinct responses to distinct mechanical stresses requires a careful design of the fluorophore in order to tune its interactions with the polymer. A series of mechanofluorochromic (MFC) polymer composites are prepared by dispersing difluoroboron diketonates complexes with various alkyl side-chain lengths (DFB-alkyl) in linear low-density polyethylene. Observation of the resulting polymer composites under a microscope reveals different aggregate sizes of the three DFB-alkyls, thus confirming the functionalization by alkyl side chains as a powerful approach to control the aggregation process in a polymer. Besides, the three polymer composite samples are shown to be sensitive to both stretching and scratching, thereby consisting in the first reported example of MFC polymer responding to these two distinct mechanical stimuli. To establish a structure–property relationship, the strategy consisted in applying controlled tensile or friction forces while simultaneously monitoring fluorescence changes. Interestingly, the intensity of the MFC response to both stretching and scratching depends on the alkyl chain length and thus on the aggregation properties of the fluorophore. According to a time-resolved fluorescence study, the emission is found to originate from different species following the type of applied stress (tensile or friction force).

1. Introduction


Among emerging smart materials, mechanofluorochromic (MFC) ones are promising for force sensing since they exhibit fluorescence modifications under external mechanical stimuli (grinding, stretching, and scratching).^[1,2] Most of the time, mechanofluorochromism originates from strain-induced perturbations of intermolecular arrangement and is reversible by solvent fuming or heating.^[3] Hence, such materials are used as local deformation probes since small fluorescence changes can be monitored in situ by common spectroscopy techniques. Stimuli-responsive materials are also potentially useful for data storage,^[4,5] mechanical printing,^[6,7] anticounterfeiting,^[8] and security purposes.^[9,10] Many molecular MFC materials, based on metal coordination complexes^[11] (in many cases of Au(I)^[12] or Pt(II))^[13] or conjugated organic molecules^[14] (like pyrene^[15] or triphenylamine),^[16] have been synthesized over the past 20 years.

Introducing such fluorophores into polymers, that are easily processable, can facilitate their handling for surface deposition and further applications.^[17] Since the pioneering work of Weder et al.,^[18] an increasing number of polymer composites have been developed^[19] by dispersing fluorophores into polymer matrices.^[20] Stilbene derivatives, such as 4,4-bis-(2-benzoxazolyl)stilbene (BBS)^[21,22] or cyano-substituted oligo(*p*-phenylene vinylene)s^[18,23] as well as perylene derivatives,^[24,25] were blended with linear low-density polyethylene (LLDPE) for instance. Covalent incorporation of fluorophores is also a promising way to achieve MFC polymers.^[26–28] Nevertheless, to date, almost all MFC polymers are sensitive to only one mechanical stimulus: the vast majority of them respond to stretching, while a few have been reported to be sensitive to compression^[29–32] or scratching.^[33,34] Moreover, to the best of our knowledge, no MFC polymer responding to both stretching and scratching has been described so far.

Highly luminescent difluoroboron β -diketonates (DFB) are known to be MFC in the powder state due to their polymorphism^[35,36] but, to date, examples of DFB-based polymers have been investigated to sense oxygen^[37,38] rather than forces. A DFB complex has already been covalently incorporated

B. Poggi, E. Lopez, R. Métivier, C. Allain
 Université Paris-Saclay
 ENS Paris-Saclay
 CNRS
 PPSM
 Gif-sur-Yvette 91190, France
 E-mail: remi.metivier@ens-paris-saclay.fr; callain@ppsm.ens-cachan.fr

L. Bodelot
 LMS
 CNRS
 École Polytechnique
 Institut Polytechnique de Paris
 Route de Saclay
 Palaiseau Cedex 91128, France
 E-mail: laurence.bodelot@polytechnique.edu

 The ORCID identification number(s) for the author(s) of this article can be found under <https://doi.org/10.1002/marc.202200134>

© 2022 The Authors. Macromolecular Rapid Communications published by Wiley-VCH GmbH. This is an open access article under the terms of the Creative Commons Attribution-NonCommercial License, which permits use, distribution and reproduction in any medium, provided the original work is properly cited and is not used for commercial purposes.

DOI: 10.1002/marc.202200134

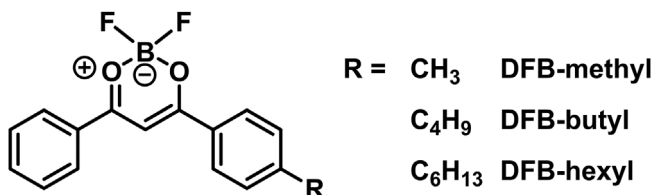


Figure 1. Structures of DFB-methyl, DFB-butyl, and DFB-hexyl.

into poly(dimethylsiloxane) (PDMS) as an energy transfer acceptor and the resulting polymer showed mechanically induced chemiluminescence upon stretching.^[39] However, DFB derivatives have never been dispersed into a polymer to trigger an MFC response. In DFB complexes, the molecular packing modes are in crystalline solids, and thus, the solid-state emission properties are governed by intermolecular interactions such as π - π stacking, hydrogen bonding, and dipole-dipole interactions.^[36,40] Moreover, studies have shown that introducing peripheral alkyl chains to organic chromophores can alter their packing modes.^[41] Fraser et al. observed that the length of alkoxy substituents on DFB influences their MFC behavior and particularly the recovery time.^[42,43] Thus, varying the length of the peripheral alkyl chain is an effective strategy to design DFB with tailored MFC properties.

Inspired by this, a series of DFB-alkyl derivatives with various alkyl side-chain lengths (-methyl, -butyl, and -hexyl) was designed and then dispersed in an LLDPE host matrix. In order to evaluate their potential as mechanical stress probes, the resulting polymer composites were first submitted to controlled tensile tests while monitoring the in situ fluorescence changes by spectroscopy. Moreover, qualitatively scratching the polymers with a spatula revealed pronounced MFC behavior. Since examples of polymers sensitive to scratching are scarce, quantification of their response to this mechanical stimulus is highly demanded. We, therefore, also focused in this study on the development of a setup able to detect fluorescence modification by both spectroscopy and imaging during the application of controlled friction forces to the polymer composites. These polymer samples were systematically observed before and after mechanical stimulation to better understand the link between aggregation states of DFB-alkyl in the polymer matrix and their MFC properties. Finally, time-resolved spectroscopy on the DFB-butyl/LLDPE polymer allowed us to unravel the different species involved in the emission before and after mechanical stimulation.

2. Results and Discussion

2.1. Synthesis and Spectroscopy in Solution

To tune the aggregation properties in the solid state, a series of three DFB derivatives with alkyl side chains of different lengths were prepared. The synthesis of DFB-methyl has been previously reported by our group (Figure 1).^[40] DFB-butyl and DFB-hexyl were synthesized via Claisen condensation of methyl benzoate with the appropriate 4'-alkylacetophenone, followed by BF_3OEt_2 mediated boron complexation with overall yields of 38% and 29%, respectively. Complete characterizations by NMR and mass spectrometry are detailed in the Supporting Information. Large

Table 1. Photophysical properties of DFB-methyl, DFB-butyl, and DFB-hexyl in THF solution.

	$\lambda_{\text{max}}(\text{abs})^{\text{a}}$ [nm]	$\lambda_{\text{max}}(\text{em})^{\text{b}}$ [nm]	ϵ^{c} [$\text{L mol}^{-1} \text{cm}^{-1}$]	$\Phi_{\text{F}}^{\text{d}}$
DFB-methyl	368	399	41300	0.32
DFB-butyl	370	400	41600	0.36
DFB-hexyl	370	401	46700	0.36

^{a)} Maximum absorption wavelength; ^{b)} Maximum emission wavelength; ^{c)} Molar absorption coefficient determined at $\lambda_{\text{max}}(\text{abs})$; ^{d)} Fluorescence quantum yield.

crystals (hundreds of micrometers in length) could be obtained for DFB-methyl, while as-synthesized DFB-butyl and DFB-hexyl are microcrystalline powders with crystallite sizes of tens of micrometers agglomerated together, as supported by the powder XRD patterns (Figure S2, Supporting Information) and the microscope images under UV irradiation (Figure S4, Supporting Information).

Photophysical properties of the DFB-alkyl were first investigated in a tetrahydrofuran (THF) solution. The three derivatives exhibit very similar UV-vis absorption and emission spectra (Figure S5, Supporting Information), and the main optical features are summarized in Table 1. Both UV-vis absorption and emission spectra display well-resolved vibronic structures with absorption maxima at 369 ± 1 nm and emission maxima at 400 ± 1 nm. The three DFB-alkyls are characterized by high molar absorption coefficients (41300 – $46700 \text{ L mol}^{-1} \text{cm}^{-1}$) and relatively high fluorescence quantum yields (0.32–0.36), which are consistent with the results previously reported for similar compounds.^[44] These results indicate that the photophysical properties of the DFB-alkyl derivatives in solution are not significantly affected by the alkyl chain length.

2.2. Solid-State Emission Properties

As expected, all the three DFB-alkyl powders exhibited MFC behavior upon grinding in a mortar (Figure S1, Supporting Information). Moreover, the fluorescence color change from cyan blue to yellow after grinding is associated with a loss of crystallinity according to powder XRD (Figure S2, Supporting Information). Photophysical properties in solid state were studied on cellulose paper substrates. The paper substrate was soaked in a concentrated solution of DFB-butyl in CH_2Cl_2 . Right after the soaking, the paper shows a purple fluorescence that is characteristic of the monomeric species in the solution (Figure 2A). A few seconds later, as the solvent starts to evaporate, a yellow emission appears and remains until ≈ 40 s. From around 50 to 90 s, the yellow fluorescence is gradually transformed into cyan blue fluorescence, and the latter finally cover the whole piece of paper. Similar behavior is observed for the papers soaked in DFB-methyl and DFB-hexyl solutions. The yellow fluorescence can be attributed to the amorphous phase, followed by the formation of the cyan crystalline state, as previously reported by Ito et al. on DFB derivatives.^[45,46] According to their study, the evaporative crystallization process follows a two-step nucleation model, where the amorphous-like state works as a precursor to nucleation. Furthermore, it has been shown on related DFB derivatives

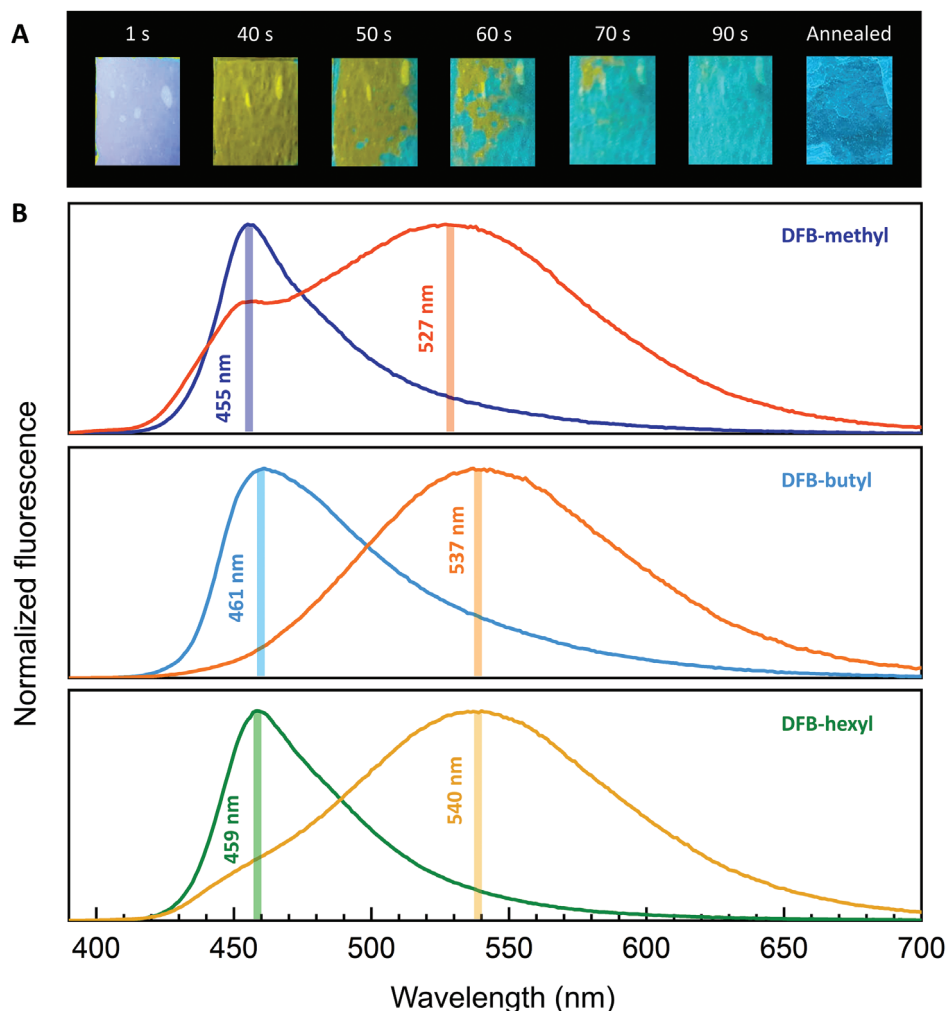


Figure 2. A) Fluorescence images ($\lambda_{\text{exc}} = 365 \text{ nm}$) after soaking a DFB-butyl solution in CH_2Cl_2 on a piece of paper. B) Emission spectra of impregnated papers with DFB-methyl, DFB-butyl, and DFB-hexyl solution in CH_2Cl_2 right after soaking (orange) and after annealing (blue/green).

that the yellow to orange fluorescence observed for the amorphous phases of such compounds was due to the formation of excimers.^[40,42] The fact that the yellow phase stays homogeneous on the paper for tens of seconds allowed us to measure its emission spectra. After soaking in DFB-alkyl solution, the impregnated papers were quickly introduced into the spectrofluorometer to acquire a spectrum of the yellow phase (orange shades in Figure 2B). Over the three derivatives, the yellow form exhibits a broad band centered around 540 nm. In the specific case of DFB-methyl, a secondary band at 455 nm is observed, which is attributed to the cyan crystalline phase that is quickly formed. This was further confirmed by the spectra of the papers thermally annealed at 100°C (blue/green shades in Figure 2B), which show a narrower band with a maximum emission of around 460 nm, for the three DFB-alkyl derivatives.

2.3. Incorporation in LLDPE

Thereafter, mechano-responsive materials based on these DFB-alkyl were developed and they are shown to be sensitive to both

stretching and scratching. DFB-alkyl was incorporated in an LLDPE host matrix with a fluorophore concentration of 1.5% w/w by solution casting method in *m*-xylene (see the detailed procedure in Supporting Information).^[25] After complete evaporation of the *m*-xylene, the three DFB-alkyl/LLDPE thin films were heated to 140°C. This final step is crucial to ensure that they are all prepared from the same state in which the fluorophore is uniformly dispersed in the melted polymer matrix. After cooling down to room temperature, the obtained polymer composite films are $\approx 200 \mu\text{m}$ thick and exhibit cyan fluorescence, suggesting the formation of DFB-alkyl crystals or crystallites in the matrix. The corresponding emission spectra present the main band with a maximum of around 460 nm, attributed to the cyan crystalline phase of the DFB-alkyl (Figure 3A). XRD measurements were performed on the polymer films and confirms the formation of the cyan crystalline phase in the LLDPE matrix (Figure S3, Supporting Information). It is worth noticing that the fluorescence emission spectrum of DFB-butyl/LLDPE is slightly broader, which is consistent with what is observed on impregnated papers and could be due to slightly different packing modes in the crystals (and possibly to a small proportion of amorphous

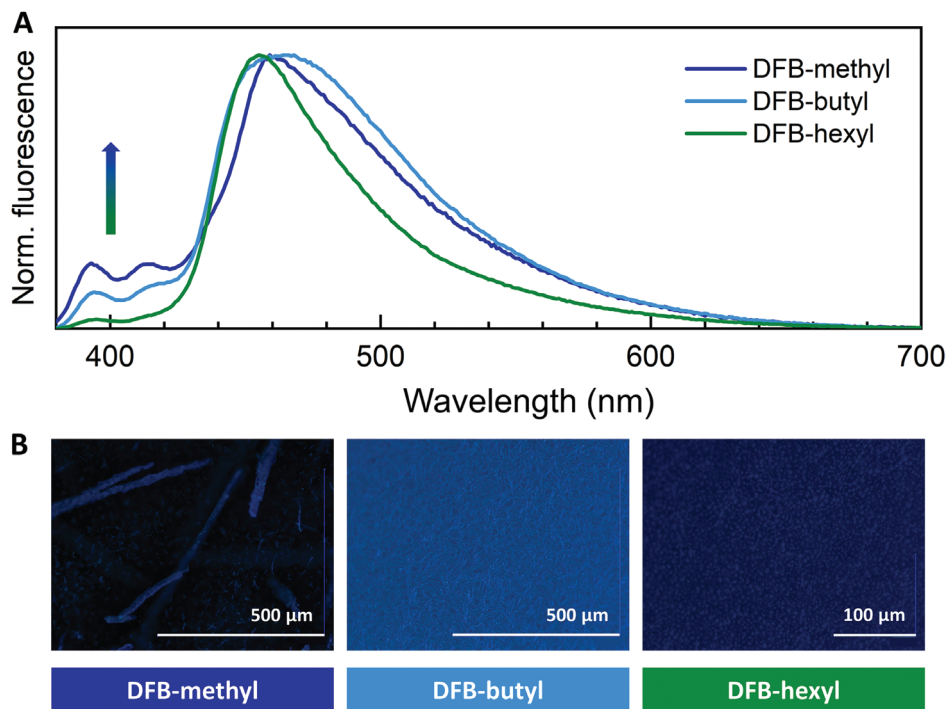


Figure 3. A) Normalized emission spectra of pristine DFB-alkyl/LLDPE samples and B) microscope fluorescence images of the corresponding polymers ($\lambda_{\text{exc}} = 365 \text{ nm}$) (a zoom is available in Figure S6, Supporting Information).

phase). Emission spectra also display two less intense bands at 397 and 417 nm, indicating the presence of monomeric DFB-alkyl in the LLDPE matrix (comparable to emission spectra in solution, see Figure S5, Supporting Information). Moreover, the intensity of this monomeric purple fluorescence contribution is decreasing from DFB-methyl to DFB-hexyl doped polymers, which is consistent with the observation made by Crenshaw et al. on cyano-substituted oligo(*p*-phenylene vinylene) derivatives.^[47] They indeed showed that increasing the alkyl side-chain length provides a higher nucleation rate, thereby leading to the formation of smaller crystallites.

To verify this hypothesis, the doped polymer samples were observed under a digital optical microscope with an excitation at 365 nm (Figure 3B and Figure S6, Supporting Information). The DFB-methyl/LLDPE sample clearly exhibits large cyan crystals with sizes in the order of hundreds of micrometers as well as smaller ones of a few micrometers on a continuous purple fluorescent background, characteristic of the monomeric emission. DFB-butyl forms tree-like crystallites with sizes from a few to tens of micrometers, while DFB-hexyl uniformly disperses in very small crystallites of micrometer scale (zoom available in Figure S6, Supporting Information). Consequently, the aggregation properties observed on the as-synthesized powders are well preserved in the LLDPE matrix. Since the DFB-methyl/LLDPE is less homogeneous, a smaller number of crystals may be in the probed area, leading to a higher proportion of monomeric species with respect to the crystals in the same probed area. On the contrary, the formed crystallites are smaller and more evenly distributed in the DFB-butyl and DFB-hexyl/LLDPE composites. Thus, the weaker contribution of the bands at 397 and 417 nm (as compared to the DFB-methyl/LLDPE sample) may arise from a

higher number of crystals in the probed area. According to the microscope images, designing DFB derivatives with alkyl side chains of various lengths is an efficient tool to control the aggregation properties in the polymer matrix.

2.4. Mechanofluorochromic Response to Stretching

The MFC response of the DFB-alkyl/LLDPE polymers to stretching was studied in a quantitative manner: quantifying the MFC response is essential to building force sensors from such materials but remains challenging. Here, the fluorescence change was monitored in situ during controlled uniaxial tensile experiments on the polymer composites (see full setup description in Supporting Information and Figure S7, Supporting Information). The samples were excited with a fibered UV source at 365 nm and the emission spectra were recorded via an optical fiber connected to a CCD-based spectrograph. Thanks to this setup, emission spectra were acquired every 5% strain up to a maximum applied nominal strain of 300%. As shown for DFB-butyl/LLDPE in Figure 4A, the bands corresponding to monomer emission gradually increase in intensity with the strain going from 0% to 200% before stabilizing upon further stretching. On the image of a manually stretched polymer sample under UV irradiation, the cyan blue fluorescence of DFB-butyl crystallites in the unstretched area (top and bottom edges) turned to purplish in the stretched area, indicating a greater contribution of the monomeric emission in the latter (Figure 4B). Much slighter change is observed on the spectra of the DFB-hexyl/LLDPE polymer upon stretching (Figure S9A, Supporting Information). On the other hand, the DFB-methyl/LLDPE sample shows a slight increase in the monomeric

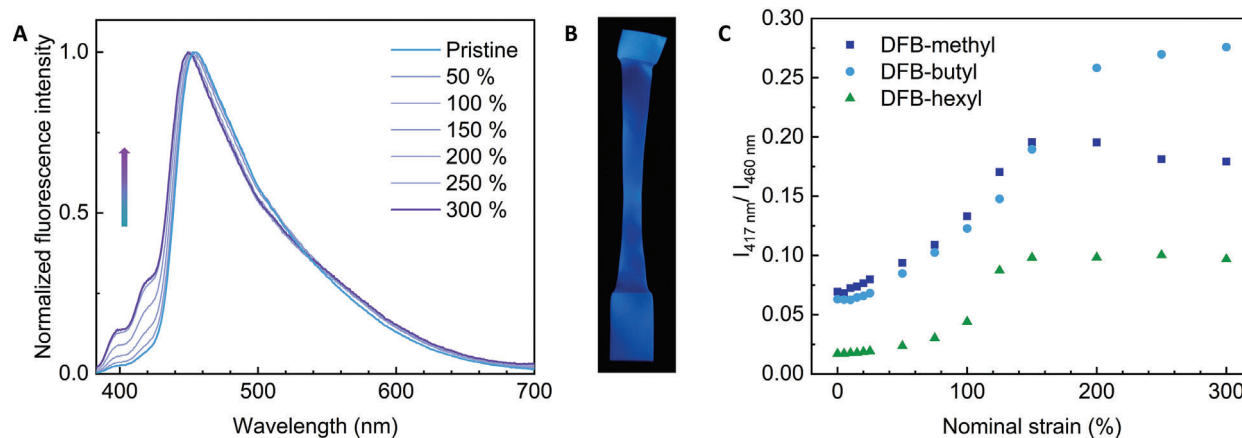


Figure 4. A) Normalized emission spectra of a DFB-butyl/LLDPE sample during controlled stretching ($\lambda_{\text{exc}} = 365$ nm), B) fluorescence image ($\lambda_{\text{exc}} = 365$ nm) after manual stretching of a DFB-butyl/LLDPE sample, and C) evolution of the normalized fluorescence intensity at 417 nm for the three DFB-alkyl/LLDPE samples.

bands around 400 nm and also in the band corresponding to the yellow phase at 540 nm (Figure S9A, Supporting Information).

According to the microscope images, the large crystals of DFB-methyl dispersed within the polymer were obviously broken by the stretching (Figures S9B and S11, Supporting Information). As a consequence, the increase of the band at 540 nm may result from the yellow phase that forms at the locations where the crystals break. For the DFB-butyl and DFB-hexyl/LLDPE samples, the crystallites are also deformed in the stretched area and oriented along the stretching direction, as evidenced by the microscope images in Figure S9B, Supporting Information. Although they look elongated by the stretching, no clear break can be observed as is the case for DFB-methyl, which could be due to their smaller size. Plotting the fluorescence intensity ratio of the 417 nm band (monomer emission) over the maximum emission band (460 nm, emission of the crystalline phase) as a function of the applied strain highlights the different responses to stretching between the three DFB-alkyl/LLDPE composites (Figure 4C). Note that a second set of tests was conducted (Figure S10, Supporting Information) and led to the same trends as those observed in Figure 4C, thereby demonstrating the reproducibility of the reported MFC behavior. As already discussed for other MFC composites,^[17,47] the MFC response of DFB-alkyl/LLDPE occurs in the plastic deformation regime since the ratio $I_{417\text{ nm}}/I_{460\text{ nm}}$ starts increasing at around 30% which is beyond the yield point, displayed in the nominal stress–strain curves (Figure S8, Supporting Information). This ratio increases up to 150% strain for DFB-methyl and DFB-hexyl/LLDPE and up to 200% strain for DFB-butyl. Then, it reaches a plateau until 300% strain for DFB-butyl and DFB-hexyl/LLDPE whereas it slightly decreases for DFB-methyl/LLDPE. Besides, the DFB-butyl/LLDPE sample obviously exhibits the highest increase of the above-mentioned ratio, even exceeding DFB-methyl/LLDPE ratio's intensity at 200% strain.

2.5. Mechanofluorochromic Response to Friction Forces

In order to investigate the response of these composite polymers to friction forces, qualitative scratching of the DFB-alkyl/LLDPE

polymers with a spatula was first performed and emission spectra as well as microscope images of the mechanically stimulated area were recorded. The fluorescence of the scratched area became yellow, evidencing a clear MFC behavior (Figure S12B, Supporting Information). Indeed, upon scratching the DFB-butyl/LLDPE sample, the emission maximum is red-shifted from 461 to 488 nm along with a strong broadening of the band (Figure S12A, Supporting Information), which is likely a convolution of the bands corresponding to blue and yellow phases. The system shows good reversibility since the pristine sample spectrum is almost recovered after exposure to *m*-xylene vapors or thermal treatment at 70°C (Figure S13, Supporting Information). On the microscope image, the tree-like crystalline structures clearly appear less sharp, implying that they were perturbed by the mechanical stimulation (Figure S12C, Supporting Information, top) that appears to be transmitted to the crystals through the polymer matrix. It is worth noting that the two bands corresponding to the monomer (397 and 417 nm) decreased in intensity after scratching but did not recover even after solvent fuming. This observation was similar to the three DFB-alkyl/LLDPE polymers.

The two other polymers doped with DFB-methyl and DFB-hexyl are also responsive to scratching as shown in Figure S12B, Supporting Information. The red-shifted band corresponding to the yellow phase also appears when they are scratched (Figure S12A, Supporting Information), and its intensity is higher (respectively lower) for DFB-methyl (respectively DFB-hexyl) than for the DFB-butyl doped polymer. In the case of DFB-methyl, the maximum wavelength of emission is even shifted to 530 nm. Moreover, this new band becomes less intense with time (spectra at 5 min and 1 h after scratching shown in Figure S12A, Supporting Information), which is due to a back reaction happening at room temperature. The kinetics of this back reaction seems to be faster with the longer alkyl chain. On the other hand, good reversibility was also obtained from DFB-methyl and DFB-hexyl/LLDPE polymers upon *m*-xylene fuming or annealing at 70°C. The microscope image of the DFB-hexyl/LLDPE polymer shows a homogeneous perturbation of the crystallites, similar to the one observed for DFB-butyl/LLDPE (Figure S12C, Supporting Information). Concerning DFB-methyl/LLDPE, the mechanical stimulus caused crystal disruption, but the partial spreading

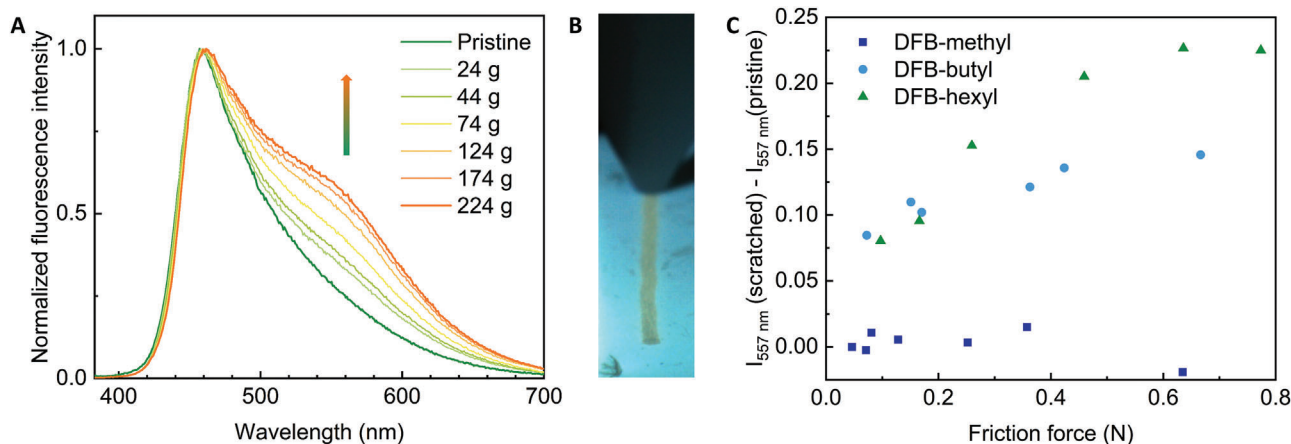


Figure 5. A) Normalized emission spectra of a DFB-hexyl/LLDPE sample during controlled scratching ($\lambda_{\text{exc}} = 365$ nm), B) corresponding fluorescence image ($\lambda_{\text{exc}} = 365$ nm) after scratching with the tip (total weight 224 g), and C) evolution of the normalized fluorescence intensity at 557 nm for the three DFB-alkyl/LLDPE samples. The y-axis corresponds to the subtraction of $I_{557\text{ nm}}$ between the spectrum after scratching and the pristine one, both measured for each experiment (i.e., at a given friction force).

of the yellow phase at the surface of the polymer resulted in a contribution of the monomer emission still visible in the spectrum. Thus, all three polymer composites exhibit a clear MFC response to qualitative scratching by a spatula.

To get a deeper insight into the relative sensitivity of the three DFB-alkyl/LLDPE composites to friction, a novel setup was specifically designed, based on the same principle as the traction one (see full setup description in the Supporting Information and Figure S14, Supporting Information). The sample, irradiated by a fibered UV source at 365 nm is scratched with a 3D printed tip pulled by a motor. A fiber connected to a CCD-based spectrograph allows to record emission spectra while scratching occurs. The intensity of the applied friction force is measured by a load cell located between the motor and the tip. Weights between 20 and 300 g were added on top of the tip (weighing itself 24 g) before each scratching experiment. According to emission spectra in Figure 5A and Figure S15A, Supporting Information, all the polymer samples exhibit an increase of intensity at 557 nm with increasing weight. As previously evidenced by the qualitative scratching, this new band corresponds to the yellow phase. In the range of forces investigated, its increase is more pronounced from DFB-methyl to DFB-hexyl composites. This trend is well confirmed by the pictures (taken with the camera) where a clear yellow mark is visible on the DFB-hexyl sample; whereas, there is no significant fluorescence color change on the DFB-methyl one (Figure 5B and Figure S15B, Supporting Information). A plot of the intensity at 557 nm ($I_{557\text{ nm}}$) versus the applied friction force highlights the higher sensitivity of DFB-hexyl/LLDPE compared to DFB-butyl/LLDPE (Figure 5C). For DFB-methyl/LLDPE, $I_{557\text{ nm}}$ stays around 0, indicating that the applied friction forces are not intense enough to induce the MFC behavior. However, the clearly visible MFC response under qualitative scratching with a spatula suggests that DFB-methyl/LLDPE is still sensitive to friction but at a higher threshold. The measured friction forces range between 0.05 and 0.77 N, thus making DFB-butyl and DFB-hexyl/LLDPE composites as much sensitive as the mechanochromic polydiacetylene-based systems developed by Oaki et al.^[48,49] (where friction forces of 0.2–23 N

were applied). In summary, the application of comparable friction forces to the three DFB-alkyl/LLDPE composites enabled the evaluation of their relative MFC response to friction and DFB-hexyl/LLDPE was found to be the most responsive one within this force range.

2.6. Time-Resolved Characterization

Finally, time-resolved fluorescence spectroscopy was performed on the DFB-butyl/LLDPE polymer to investigate the emissive species involved in the pristine, stretched, and scratched samples. The fluorescence decays were recorded at 395, 460, and 580 nm emission wavelengths, corresponding to the emission from the monomers (purple), the cyan blue, and the yellow phases, respectively (Figure S16, Supporting Information). All the decay curves were fitted using a discrete multi-exponential decay model and a global analysis of the three samples for each wavelength successfully converged (Global $\chi^2 < 1.2$). Four components were necessary to fit the fluorescence decays, indicating a complex system where many species contribute to the emission in different proportions. The decay-times τ_i and corresponding pre-exponential factors a_i are summarized in Table S1, Supporting Information. The intermediate decay-time τ_2 (0.86 ns) at an emission wavelength of 395 nm, which represents the major component of the pristine sample, is attributed to the monomeric fluorescence. Indeed, a solution of DFB-butyl in THF provided a mono-exponential decay defined by a lifetime of 0.80 ns. This confirms the presence of emitting monomers in the polymer samples. The shortest component τ_1 (0.20–0.39 ns) is associated with negative pre-exponential factors for the longer wavelength emission at 580 nm. Moreover, the longest component τ_4 (13.32–29.68 ns) represents a high contribution with a positive pre-exponential factor at an emission of 580 nm, especially for the scratched sample. Therefore, the rise time observed at short decay time, combined with the emerging long-time component at 580 nm suggests the formation of excimers (or possibly the presence of energy transfer processes) in the yellow phase

obtained upon scratching of the DFB-butyl/LLDPE polymer. This is fully consistent with our previous observations on DFB derivatives studied as pure molecular materials^[40,50] and suggests that the friction force is efficiently transmitted to the DFB compound through the polymer matrix.

3. Conclusion

We herein presented the design and synthesis of DFB-alkyl derivatives with alkyl side-chain lengths going from methyl to hexyl. As expected, they all display similar photophysical properties in solution as well as in the solid state, for which three distinct emissive contributions, purple monomer, cyan blue crystalline phase, and yellow amorphous phase, were evidenced. Successful incorporation of the DFB-alkyl by dispersion in LLDPE provided polymer composites with different aggregation behaviors according to the chain length. All DFB-alkyl/LLDPE samples show MFC response to both manual stretching and scratching with a spatula, which is unprecedented according to the literature. Investigation of the samples by steady-state and time-resolved fluorescence spectroscopies, as well as microscopy, provided useful information about the different emissive species at stake before and after mechanical stimulation. Stretching induces mainly an increase in the monomeric emission compared to the initial cyan blue fluorescence, whereas scratching results in the appearance of a yellowish emission involving excimers or energy transfer. The polymer composites were finally submitted to controlled tensile and friction forces while monitoring the fluorescence modification by in situ spectroscopy. Thanks to these two experimental setups, the intensity of the MFC response to both mechanical stimuli has been quantitatively evaluated for the three DFB-alkyl/LLDPE polymers. In the range of applied forces in this study, DFB-butyl/LLDPE composite was found to be the most sensitive to stretching, whereas the DFB-hexyl/LLDPE one exhibits the greatest MFC response to friction. This work revealed that DFB derivatives embedded in LLDPE are able to detect different mechanical stimuli, such as stretching or scratching stresses, with distinct fluorescence responses, thus making them suitable as mechanical stress probes, and constituting a step forward toward the use of fluorescence to quantify mechanical stress on polymer objects undergoing complex mechanical stimulations. From this perspective, the combined effects of stretching and scratching on a given sample could also be studied.

Supporting Information

Supporting Information is available from the Wiley Online Library or from the author.

Acknowledgements

This project had received funding from the European Research Council (ERC) under the European Union's Horizon 2020 research and innovation program (grant agreement No 715757 MECHANO-FLUO to C.A.) and from the Mission pour l'Interdisciplinarité du CNRS (défi "Mécanobio"). L.B. acknowledges that this research benefited, through the use of the PLATINE platform, from the support of the École Polytechnique fund raising—Smart environments: Nanosensors and Nanoreliability Initiative.

Erik Guimbretière, Pascal Marie, and Vincent de Greef, at LMS, are acknowledged for, respectively, contributing to the design of the setup, machining the parts, and adapting the Agnes software to the new setup. The authors gratefully acknowledge Arnaud Brosseau (PPSM) and Dr. Oleksandr Pasko (SATIE) for their help with the time-resolved fluorescence measurements and powder XRD analyses, respectively.

Conflict of Interest

The authors declare no conflict of interest.

Data Availability Statement

The data that support the findings of this study are available in the Supporting Information of this article.

Keywords

controlled mechanical stimuli, fluorescence, force sensors, mechano-responsive materials, phase transformation, polymers

Received: February 15, 2022

Revised: April 6, 2022

Published online:

- [1] Y. Sagara, T. Kato, *Nat. Chem.* **2009**, *1*, 605.
- [2] D. Yan, D. G. Evans, *Mater. Horiz.* **2014**, *1*, 46.
- [3] C. Wang, Z. Li, *Mater. Chem. Front.* **2017**, *1*, 2174.
- [4] H. Sun, S. Liu, W. Lin, K. Y. Zhang, W. Lv, X. Huang, F. Huo, H. Yang, G. Jenkins, Q. Zhao, W. Huang, *Nat. Commun.* **2014**, *5*, 3601.
- [5] Y. Hou, Z. Li, J. Hou, P. Shi, Y. Li, M. Niu, Y. Liu, T. Han, *Dyes Pigm.* **2018**, *159*, 252.
- [6] P. Shi, D. Deng, C. He, L. Ji, Y. Duan, T. Han, B. Suo, W. Zou, *Dyes Pigm.* **2020**, *173*, 107884.
- [7] Z. Yu, Y. Zhang, C. Wang, X. Du, H. Lu, Q. Wang, *Dyes Pigm.* **2021**, *190*, 109342.
- [8] Z. Man, Z. Lv, Z. Xu, Q. Liao, J. Liu, Y. Liu, L. Fu, M. Liu, S. Bai, H. Fu, *Adv. Funct. Mater.* **2020**, *30*, 2000105.
- [9] V. C. Wakchaure, T. Das, S. S. Babu, *ChemPlusChem* **2019**, *84*, 1253.
- [10] V. K. Praveen, B. Vedhanarayanan, A. Mal, R. K. Mishra, A. Ajayaghosh, *Acc. Chem. Res.* **2020**, *53*, 496.
- [11] X. Zhang, Z. Chi, Y. Zhang, S. Liu, J. Xu, *J. Mater. Chem. C* **2013**, *1*, 3376.
- [12] H. Ito, T. Saito, N. Oshima, N. Kitamura, S. Ishizaka, Y. Hinatsu, M. Wakeshima, M. Kato, K. Tsuge, M. Sawamura, *J. Am. Chem. Soc.* **2008**, *130*, 10044.
- [13] D. Genovese, A. Aliprandi, E. A. Prasetyanto, M. Mauro, M. Hirtz, H. Fuchs, Y. Fujita, H. Uji-I, S. Lebedkin, M. Kappes, L. De Cola, *Adv. Funct. Mater.* **2016**, *26*, 5271.
- [14] Z. Chi, X. Zhang, B. Xu, X. Zhou, C. Ma, Y. Zhang, S. Liu, J. Xu, *Chem. Soc. Rev.* **2012**, *41*, 3878.
- [15] Y. Sagara, T. Mutai, I. Yoshikawa, K. Araki, *J. Am. Chem. Soc.* **2007**, *129*, 1520.
- [16] P. S. Hariharan, D. Moon, S. P. Anthony, *J. Mater. Chem. C* **2015**, *3*, 8381.
- [17] F. Ciardelli, G. Ruggeri, A. Pucci, *Chem. Soc. Rev.* **2013**, *42*, 857.
- [18] C. Löwe, C. Weder, *Adv. Mater.* **2002**, *14*, 1625.
- [19] A. Pucci, R. Bizzarri, G. Ruggeri, *Soft Matter* **2011**, *7*, 3689.
- [20] A. Pucci, G. Ruggeri, *J. Mater. Chem.* **2011**, *21*, 8282.
- [21] A. Pucci, C. Cappelli, S. Bronco, G. Ruggeri, *J. Phys. Chem. B* **2006**, *110*, 3127.

- [22] A. Battisti, P. Minei, A. Pucci, R. Bizzarri, *Chem. Commun.* **2017**, 53, 248.
- [23] B. R. Crenshaw, C. Weder, *Chem. Mater.* **2003**, 15, 4717.
- [24] F. Donati, A. Pucci, C. Cappelli, B. Mennucci, G. Ruggeri, *J. Phys. Chem. B* **2008**, 112, 3668.
- [25] A. Pucci, F. Donati, G. Ruggeri, F. Ciardelli, *E-Polymers* **2009**, 9, 058.
- [26] B. R. Crenshaw, C. Weder, *Macromolecules* **2006**, 39, 9581.
- [27] H. Traeger, Y. Sagara, D. J. Kiebal, S. Schrettl, C. Weder, *Angew. Chem., Int. Ed.* **2021**, 60, 16191.
- [28] S. He, M. Stratigaki, S. P. Centeno, A. Dreuw, R. Göstl, *Chem. - Eur. J.* **2021**, 27, 15889.
- [29] D. A. Davis, A. Hamilton, J. Yang, L. D. Cremer, D. Van Gough, S. L. Potisek, M. T. Ong, P. V. Braun, T. J. Martínez, S. R. White, J. S. Moore, N. R. Sottos, *Nature* **2009**, 459, 68.
- [30] J. Kunzleman, M. Gupta, B. R. Crenshaw, D. A. Schiraldi, C. Weder, *Macromol. Mater. Eng.* **2009**, 294, 244.
- [31] C. Calvino, A. Guha, C. Weder, S. Schrettl, *Adv. Mater.* **2018**, 30, 1704603.
- [32] C. Calvino, E. Henriët, L. F. Muff, S. Schrettl, C. Weder, *Macromol. Rapid Commun.* **2020**, 41, 1900654.
- [33] J. R. Kumpfer, S. D. Taylor, W. B. Connick, S. J. Rowan, *J. Mater. Chem.* **2012**, 22, 14196.
- [34] S.-J. Yoon, J. W. Chung, J. Gierschner, K. S. Kim, M.-G. Choi, D. Kim, S. Y. Park, *J. Am. Chem. Soc.* **2010**, 132, 13675.
- [35] G. Zhang, J. Lu, M. Sabat, C. L. Fraser, *J. Am. Chem. Soc.* **2010**, 132, 2160.
- [36] P.-Z. Chen, L.-Y. Niu, Y.-Z. Chen, Q.-Z. Yang, *Coord. Chem. Rev.* **2017**, 350, 196.
- [37] C. A. DeRosa, J. Samonina-Kosicka, Z. Fan, H. C. Hendargo, D. H. Weitzel, G. M. Palmer, C. L. Fraser, *Macromolecules* **2015**, 48, 2967.
- [38] C. A. DeRosa, S. A. Seaman, A. S. Mathew, C. M. Gorick, Z. Fan, J. N. Demas, S. M. Peirce, C. L. Fraser, *ACS Sens.* **2016**, 1, 1366.
- [39] Y. Yuan, B. Di, Y. Chen, *Macromol. Rapid Commun.* **2020**, 42, 2000575.
- [40] L. Wilbraham, M. Louis, D. Alberga, A. Brosseau, R. Guillot, F. Ito, F. Labat, R. Métivier, C. Allain, I. Ciofini, *Adv. Mater.* **2018**, 30, 1800817.
- [41] S. Xue, X. Qiu, Q. Sun, W. Yang, *J. Mater. Chem. C* **2016**, 4, 1568.
- [42] N. D. Nguyen, G. Zhang, J. Lu, A. E. Sherman, C. L. Fraser, *J. Mater. Chem.* **2011**, 21, 8409.
- [43] W. A. Morris, M. Sabat, T. Butler, C. A. DeRosa, C. L. Fraser, *J. Phys. Chem. C* **2016**, 120, 14289.
- [44] Y. N. Kononevich, I. B. Meshkov, N. V. Voronina, N. M. Surin, V. A. Sazhnikov, A. A. Safonov, A. A. Bagaturyants, M. V. Alfimov, A. M. Muzafarov, *Heteroat. Chem.* **2013**, 24, 271.
- [45] F. Ito, M. Saigusa, N. Kanayama, *Chem. Lett.* **2019**, 48, 1199.
- [46] F. Ito, *Symmetry* **2020**, 12, 1726.
- [47] B. R. Crenshaw, M. Burnworth, D. Khariwala, A. Hiltner, P. T. Mather, R. Simha, C. Weder, *Macromolecules* **2007**, 40, 2400.
- [48] H. Terada, H. Imai, Y. Oaki, *Adv. Mater.* **2018**, 30, 1801121.
- [49] K. Watanabe, H. Imai, Y. Oaki, *J. Mater. Chem. C* **2020**, 8, 1265.
- [50] M. Louis, A. Brosseau, R. Guillot, F. Ito, C. Allain, R. Métivier, *J. Phys. Chem. C* **2017**, 121, 15897.